Numerical analysis of the wake of a 10kW HAWT

S G Gong[1], Y B Deng, G L Xie and J P Zhang

School of Mechanical Engineering, Xiangtan University, Xiangtan, Hunan, 411105, China

E-mail: gongsg@xtu.edu.cn

Abstract: With the rising of wind power industry and the ever-growing scale of wind farm, the research for the wake performance of wind turbine has an important guiding significance for the overall arrangement of wind turbines in the large wind farm. The wake simulation model of 10kW horizontal-axis wind turbine is presented on the basis of Averaged Navier-Stokes (RANS) equations and the RNG k-ε turbulence model for applying to the rotational fluid flow. The sliding mesh technique in ANSYS CFX software is used to solve the coupling equation of velocity and pressure. The characters of the average velocity in the wake zone under rated inlet wind speed and different rotor rotational speeds have been investigated. Based on the analysis results, it is proposed that the horizontal spacing between the wind turbines is less than two times radius of rotor, and its longitudinal spacing is less than five times of radius. And other results have also been obtained, which are of great importance for large wind farms.

1. Introduction

Flow analysis of wind turbine wake has been one of the important subjects in the field of aerodynamics. Researchers have studied the influence of wind turbine wake on wind turbine design and performance [1-2], for example, in large offshore wind farm, average power loses due to wind turbine wakes are of the order of 10 to 20% of total power output. The power of wind turbine can be impacted by the velocity distribution of wind turbine wake zone. Specially, the near-wake velocity will affect the aerodynamic loading on the blade, and the far-wake velocity will have direct effect on the output power of downstream wind turbines [3].

The wake distribution of Horns Rev large offshore wind farm was simulated and analyzed by computing through the computational fluid dynamics (CFD), and further compared with measures data of wind farm have been finished. The research results indicate that wind farm models require modification to reduce under-prediction of wake losses while CFD models typically over-predict wake losses [4]. Sarlak, et al [5] studied the wake and power characteristics of a horizontal-axis wind turbine in a wind tunnel, and their results demonstrate how the blockage effect increases with the tip speed ratio. Sarmast, et al [6] has investigated the wake interaction between two model scale wind turbines with span-wise offset by using Large Eddy Simulation. The results show that the rotor characteristics for both rotors are well captured numerically even if the downstream rotor operates into stall regimes. The near-wake velocity field of a model horizontal-axis wind turbine (HAWT) has been calculated with different tip speed ratios, and the distributions of the near-wake velocity behind the HAWA rotor were obtained [7]. Wang, et al [8] has studied the wake of wind turbine under the stochastic wind field, and indicated that the wind turbine wake tip vortex line appeared serious distortion and asymmetry. Zhou, et al. [9] employed Weissinger-L lifting surface model with a time-marching free vortex methodology to compute the effect of steady wind shear and transient dynamic inflow wind on the wake structure and performance characteristics of a HAWT rotor. In experimental aspect, Hu, et al.

[10] utilized wind tunnel experimental model to study the influence of the different incoming wind speed and turbulence intensity on the wind turbine wake. Gao, et al. [11] have carried out the measure of velocity field in near wake of HAWT by using cross correlation Particle Image Velocimetry (PIV) and axis-coder positioning period sampling system at wind tunnel opening. Zhang, et al. [12] have collected the wake stream data as far as 4.5 times of the rotor diameter in wind turbine downstream by using TR-PIV, and found that the dissipation speed of the tip vortex is faster than the center vortex and the leapfrogging phenomenon of the tip vortex. Lignarolo, et al. [13] have investigated the vortical structures of the wake of a HAWT model by stereoscopic PIV, and their research indicated that the wake instability has a strong impact on the momentum deficit recovery of the wake. Many research results about the wind turbine wake and performance have acquired, but for a specific wind turbine, the wind turbine wake and its performance need to be further confirmed.

In this paper, the wake flow for 10 kW HAWT will be simulated by using sliding mesh technology and RNG k-ε turbulence model that apply to rotate fluid analysis. The wake flow field of wind turbine under different wind rotor velocity is studied. The results obtained are considered to be highly helpful in the design and installation of 10kW HAWT.

2. Computing Model

The design parameter of 10kW HAWT is given in the Table 1, and the geometric parameter of blades are shown in the Table 2.

Table 1. design parameter of HAWT

Rated power (kW)	Rated wind speed(m/s)	Cut-in wind speed(m/s)	Cut-out wind speed (m/s)	Number of blades	Rotor diameter(m)	Rated rotor speed (rpm)
10	10	3.2	16	3	8	180

Table 2. geometric parameter of blades

Section	Span(m)	Chord(m)	Torsional angle	Profoil
1	0	0.2	14.6413	Cylinder
2	0.4	0.2	14.6413	Cylinder
3	0.8267	0.5298	14.6413	SG6040
4	1.0533	0.4763	12.0487	SG6040
5	1.2800	0.4169	9.6188	SG6040
6	1.5067	0.3665	7.6366	SG6040
7	1.7333	0.3257	6.0381	SG6040
8	1.9600	0.2923	4.7485	SG6040
9	2.1867	0.2649	3.6922	SG6040
10	2.4133	0.2422	2.8095	SG6040
11	2.6400	0.2229	2.0633	SG6040
12	2.8667	0.2066	1.4184	SG6040
13	3.0933	0.1923	0.8454	SG6040
14	3.3200	0.1796	0.3107	SG6040
15	3.5467	0.1671	-0.2293	SG6040
16	3.7733	0.1516	-0.9051	SG6040
17	4.0000	0.0000	0.6946	SG6040

The three blades model of 10kW HAWT obtained by using data in the Table 2 is shown as Figure 1, and the three-dimension numerical model of wind turbine is also shown as Figure 2. The model in Figure 2 is divided into 3.8 million grids, in which the mesh smoothing is achieved and the local refinement near the surface of blade is adopted. The grid model of computed field and near the surface of blade is shown as Figure 3, Figure4, respectively.

The boundary conditions are given as follow: Inlet velocity is v=10m/s. The rotor rotational speed of blade is 180rpm, and outlet pressure is the average static pressure. The surface of blade is set to no slipping and impermeable boundary condition. The wind flow is defined as the axis free flow under the steady condition. The convergence error is set to 10^{-5}.

For considering the influence of blade rotation effect on airfoil performance, the simulation of 3D aerodynamic performance of 10kW HAWT is achieved by using sliding mesh unsteady computing method and based on the 3D *Navier-stokes equation* and *RNG k-ε turbulence model*. The pressure implicit split operator in SIMPLE algorithm is used to solve the coupling equation of pressure and velocity. The pressure item is discretized by the PRESTO format. The overall computing time is set to 28s, and the time step is 0.0028s.

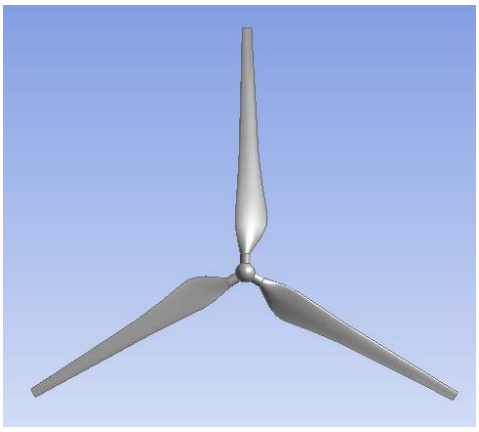

Figure 1. Geometric model of wind rotor

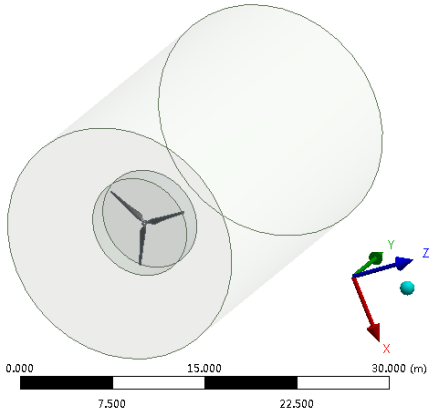

Figure 2. The computing model

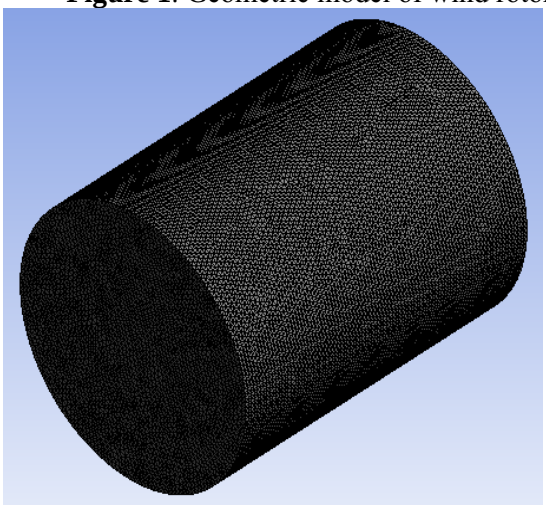

Figure 3. Overall grid of computed field

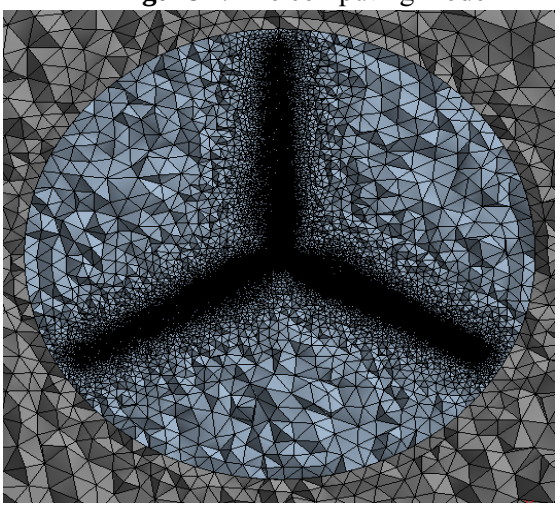

Figure 4. Grid near the surface of blade

3. Simulated results and analysis

3.1. The wake of under rated condition

The wake feature of the wind turbine is obtained by simulated computing under rated condition, that is: rated wind velocity is 10m/s and rated rotor speed is 180rpm. The average wind speed contour slice of the wake field of wind turbine in different along-wind location is shown in Figure 5.

In Figure 5, we can find that the average wind velocity contours begin to change in the 5r (r is radius of wind rotor) location of the wake region, and while the wind come to the seven times rotor

radius location, the distribution of velocity contour have a great change. When the distance of wake reaches 9*r*, the contour distribution of wind velocity is close to the one of incoming flow.

The curve of cross-wind average wind speed in the different location of wake field is shown as Figure 6. The cross-wind average wind velocity in the 2*r* and 3*r* location of the wake field has a sharp change. The minimum cross-wind average wind speed in the center of wind rotor is 0.1 times of inflow wind speed, and it is mainly concentrated in range of +/- 1.5*r*. The main reason of change is that the flow is affected by the wind wheel rotation and wheel hub. As the wake area increases to 6*r*, the cross-wind involved area of the wake have been expanded upward to +/- 2.5*r*, but the minimum cross-wind velocity increase gradually 0.8 times of inflow wind. When the wake region continues to increase to 10*r*, the average cross-wind velocity is close to the inflow wind speed, that is, the flow field of whole area has been basically no longer affected by the wind wheel rotation.

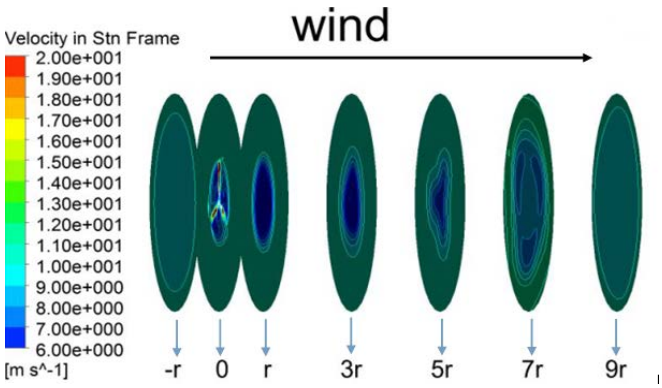

Figure 5. The average wind speed contour slice in the wake field along-wind location

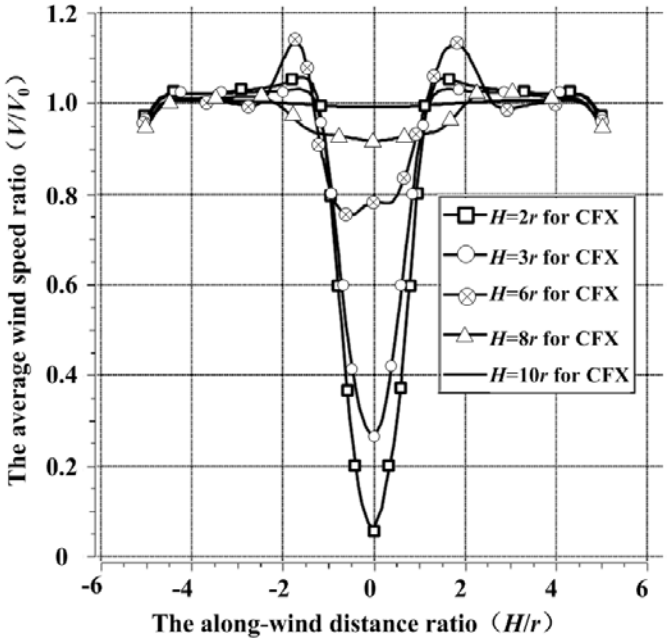

Figure 6. The average wind speed of cross-wind in the wake area

Based on the above analysis, we can obtain that the arrangement between wind turbines in the wind farm considers not only the situation of local wind resource, and also think about the influence of horizontal spacing and longitudinal spacing between the wind turbines, so as to reduce the impacts of the wake on its two sides and downstream wind turbine. Thus, we suggest that the horizontal spacing and longitudinal spacing between the wind turbines is less than 4*r* and 10*r*, respectively, in the installation of 10kW HAWT.

3.2. The wake under different wind rotational speed

In order to study on the influence of wind wheel rotation speed on the wake flow and aerodynamic performance of wind turbine, while the velocity of incoming flow is 10m/s, and the velocity of rotation is 80rpm, 120rpm, respectively, the simulation analysis based on the model shown in Figure 2 is achieved. The change curve of the along-wind average wind speed in the wake area is obtained, and the results are shown in Figure 7.

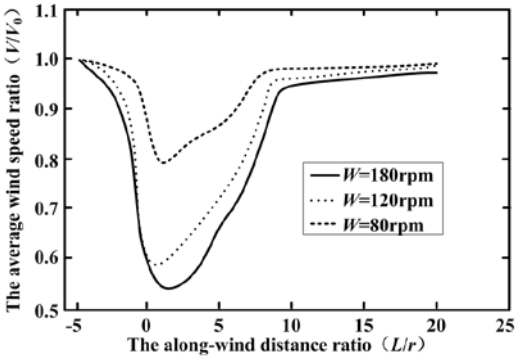

Figure 7. The curve of the along-wind average wind speed in wake area

As we can see in Figure 7, the average wind speed in the same location of the wake area is decreased obviously as the wind wheel rotation velocity increase, especially from 80rpm to 120rpm, the greater the rotation speed is, the more significant the influence of it on the rear wind turbine is. While the rotation speed increase from 120rpm to 180rpm, the growth of average wind velocity becomes slower with rotation speed increase. It indicates that the effect of the rotation speed increase on the wake flow will no longer be visible as the rotation speed of rotor reaches a certain value.

The curve of the along-wind pressure factor in the rotor wake area is shown in Figure 8 under different wind wheel rotation speed. We can find in Figure 8 that the pressure factor after and before wind wheel is increasing with the rotation speed increase. This is mainly reason why the blade tip speed ration will be enlarged with increase of rotational speed, and gradually close to its optimal value.

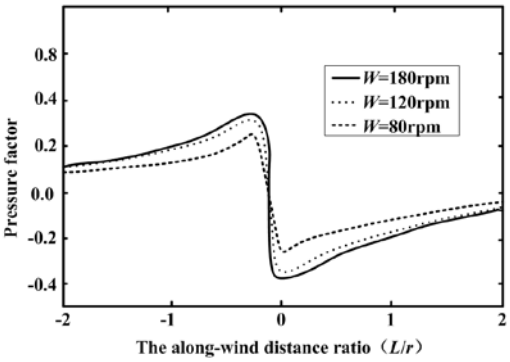

Figure 8. The pressure factor of the along-wind in the wake area

In order to quantify the influence of rotor speed on the cross-wind in the wake area, the cross-wind speed curve in the section that is 3*r* and 8*r* distant from the wind rotor in the wake area is obtained, respectively, as shown in Figure 9 and Figure 10.

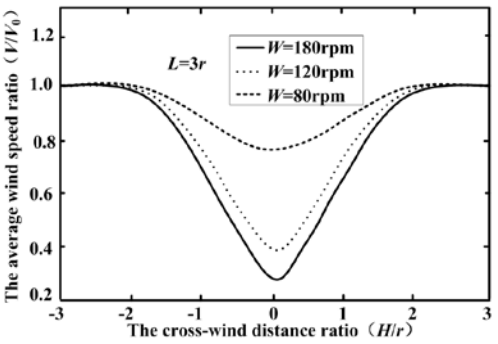

Figure 9. The cross-wind average speed as the distance is 3*r*

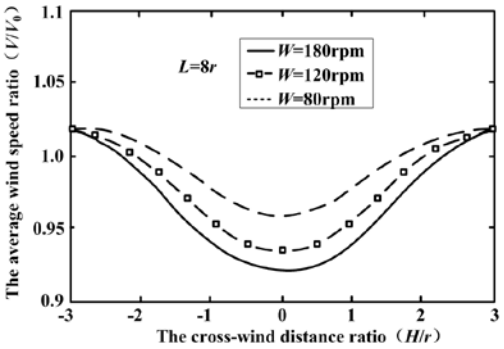

Figure 10. The cross-wind average speed as the distance is 8*r*

As shown in Figure 9 and Figure 10, when the rotor rotational speed increases from 80rpm to 120rpm, that is, the tip speed ratio increases from 3.45 to 5.02, the cross-wind average speed ration in 3*r* section decline significantly, and its minimum value decrease from 0.8 to 0.4. However, when the distance between the cross-section and rotor is 8*r*, the cross-wind average speed ratio decline is not quite obvious, but the affected cross-wind range compared with 3r section is increased. The mean wind speed ration in the given section will go on decreasing as the rotor rotational speed increase to 180rpm, but it decreases at a slowly rate and the affected cross-wind range also remain unchanged.

4. Conclusion

The conclusion can be obtained by simulation analyzing of the wake flow for 10kW HAWT, and it is given as follows.

(1) Based on *Reynolds Averaged Navier-Stokes* equations and RNG k-ε turbulence model for rotational flow analysis, the wake flow analysis under the rated operating condition is achieved. Through the analysis of average wind speed in the wake field, it is proposed that the horizontal spacing between the wind turbines is less than 4*r*, and its longitudinal spacing is less than10*r*.

(2) By simulation analyzing for the wake flow under different rotor rotational speed, the influence of the rotor rotational speed on the wake flow is obtained. It is beneficial to optimize the relation of rotor rotational speed with transverse and longitudinal spacing between the wind turbines.

Acknowledgment

This research is funded by National Natural Science Foundation of China [51375417, 51405415], and the financial support to the first author is gratefully acknowledged.

References

[1] Hu Danmei, Ou Yanghua and Du Zhaohui 2006 *Acta Energi. Sin*. **27** 606-612
[2] Vermeer L J, Screusen J N and Crespo A 2003 *Prog. Aerosp. Sci.* **396** 467-5l0
[3] Whale J and Anderson C G 2000 *J. Wind Eng. Ind. Aerod.* **84** 1-21
[4] Barthelmle R J, Hansen K, Schepers J G, et al 2009 *Wind Energ.* **12** 431-444
[5] Sarlak H, Nishino T, Martínez tossas L A, et al 2016 *Renew. Energ*. **93** 340-352
[6] Sarmast S, Chivaee H S, Ivanell S, et al. 2014 *J. Phys. Conf.* **524** 012137
[7] Hu Danmei, Zhang Jianping 2010 *Acta Energi. Sin*. **31** 1485-1490
[8] Wang Xiao, Cao Jiufa and Wang Tongguang 2016 *Chin. J. Comput. Mech.* **33** 343-350
[9] Zhou Wenping, Tang Shengli and Lu Hong 2012 *Proc. CSEE* **32** 122-127
[10] Hu Danmei and Du Zhaohui 2009 *J. Hydrodyn.* **21** 285-291
[11] Gao Zhiying, Wang Jianwen, Dong Xueqing, et al. 2011 *Acta Energi. Sin*. **32** 897-900
[12] Zhang Shucheng, Dong Xueqing, Wang Jianwen, et al. 2016 *J.Eng. Thermophy*. **37** 1432-1437
[13] Lignarolo LEM, Ragni D, Krishnaswami C, et al. 2014 *Renew. Energ*. **70** 31-46